3-2014

Seasonal Evapotranspiration Patterns in Mangrove Forests

Jordan G. Barr
South Florida Natural Resource Center, Everglades National Park, jordan_barr@nps.gov

Marcia S. DeLonge
University of California - Berkeley

Jose D. Fuentes
Pennsylvania State

Recommended Citation
Barr, J.G., M.S. DeLonge, J.D. Fuentes. 2014. Seasonal evapotranspiration patterns in mangrove forests. Journal of Geophysical Research: Atmospheres 119(7): 3886-3899. DOI: 10.1002/2013JD021083

This material is based upon work supported by the National Science Foundation through the Florida Coastal Everglades Long-Term Ecological Research program under Cooperative Agreements #DBI-0620409 and #DEB-9910514. Any opinions, findings, conclusions, or recommendations expressed in the material are those of the author(s) and do not necessarily reflect the views of the National Science Foundation.

AGU PUBLICATIONS

JGR

Journal of Geophysical Research: Atmospheres

RESEARCH ARTICLE
10.1002/2013JD021083

Key Points:
- Forests partitioned energy like semi-arid environments during the dry season
- Increased salinity reduced evapotranspiration (ET) by as much as 26%
- Site-specific models reproduced seasonal rates of ET in mangrove forests

Correspondence to:
J. G. Barr,
Jordan_Barr@nps.gov

Citation:
Barr, J. G., M. S. DeLonge, and J. D. Fuentes (2014), Seasonal evapotranspiration patterns in mangrove forests, *J. Geophys. Res. Atmos.*, *119*, doi:10.1002/2013JD021083.

Received 23 OCT 2013
Accepted 9 MAR 2014
Accepted article online 13 MAR 2014

Seasonal evapotranspiration patterns in mangrove forests

Jordan G. Barr[1], Marcia S. DeLonge[2], and Jose D. Fuentes[3]

[1]South Florida Natural Resource Center, Everglades National Park, Homestead, Florida, USA, [2]Department of Environmental Science, Policy, and Management, University of California, Berkeley, California, USA, [3]Department of Meteorology, Pennsylvania State University, University Park, Pennsylvania, USA

Abstract Diurnal and seasonal controls on water vapor fluxes were investigated in a subtropical mangrove forest in Everglades National Park, Florida. Energy partitioning between sensible and latent heat fluxes was highly variable during the 2004–2005 study period. During the dry season, the mangrove forest behaved akin to a semiarid ecosystem as most of the available energy was partitioned into sensible heat, which gave Bowen ratio values exceeding 1.0 and minimum latent heat fluxes of 5 MJ d^{-1}. In contrast, during the wet season the mangrove forest acted as a well-watered, broadleaved deciduous forest, with Bowen ratio values of 0.25 and latent heat fluxes reaching 18 MJ d^{-1}. During the dry season, high salinity levels ($>$ 30 parts per thousand, ppt) caused evapotranspiration to decline and correspondingly resulted in reduced canopy conductance. From multiple linear regression, daily average canopy conductance to water vapor declined with increasing salinity, vapor pressure deficit, and daily sums of solar irradiance but increased with air temperature and friction velocity. Using these relationships, appropriately modified Penman-Monteith and Priestley-Taylor models reliably reproduced seasonal trends in daily evapotranspiration. Such numerical models, using site-specific parameters, are crucial for constructing seasonal water budgets, constraining hydrological models, and driving regional climate models over mangrove forests.

1. Introduction

Despite their location in regions with the greatest energy and water availability on Earth, mangrove forests exhibit transpiration rates that can be as low as in semiarid environments [*Ball*, 1986, 1988; *Passioura et al.*, 1992]. Unlike other vegetated systems, mangrove forests need to obtain water from highly saline sources while being exposed to high levels of radiation and evaporative demand. The high carbon and energetic costs of salt exclusion requires that mangrove trees use water conservatively despite its abundance [*Ball*, 1988]. These conditions imply that mangrove forests are water stressed. Therefore, regional transpiration rates from these forest canopies may be regulated more by plant stomata than by meteorological conditions. Surface-vegetation-atmosphere transfer models principally focus on atmospheric conditions and can require careful adjustment when applied to different land cover types [*Choi et al.*, 2012]; current models do not consider the primary factor of the water stress on stomatal conduction and thus evapotranspiration in mangroves induced by high salinity levels. At high salinity levels, stomatal conductance may be less than predicted by plant models that are based on local climate variables. Thus, relationships between stomatal conductance and environmental drivers are needed to ensure that mangrove forests are reliably represented in weather and climate models. At a minimum, typical ranges of canopy conductance to water vapor must be quantified for mangrove forests.

Mangrove forests are pan-tropical and cover a global area of approximately 138,000 km^2 [*Giri et al.,* 2011] of coastal and riverine environments. These forests have a year-round growing season and an annual net primary productivity of 218 ± 72 Tg C [*Bouillon et al.,* 2008]. Mangrove roots are frequently exposed to saline or brackish water and need to secrete, exclude, or accumulate the salt from the water [*Parida and Jha*, 2010]. Their roots maintain continuous water uptake and regulate ion uptake against a salt gradient [*Ball*, 1996; *Parida and Jha*, 2010] where osmotic potentials can exceed that of seawater, −2.5 MPa [*Sperry et al.*, 1988]. Such energetic costs often necessitate minimizing water loss through reduced stomatal conductance and transpiration rates [*Ball and Farquhar*, 1984]. Mangrove forests are particularly susceptible to water loss during periods with high radiational loads or high vapor pressure deficit (VPD). To keep leaves cool without drastically reducing photosynthesis, mangrove trees have adapted to change leaf angles, decrease leaf size, and enhance leaf succulence [*Ball et al.,* 1988]. To sufficiently limit water loss, however, mangrove trees also

minimize stomatal conductance, assimilating more carbon per unit water loss; therefore, mangrove forests exhibit water use efficiency (WUE, ratio of carbon gain to water loss) greater than the majority of C_3 plants [*Ball,* 1986; *Ball et al.,* 1988]. While mangrove species exhibit different degrees of salt tolerance and WUE, increasing salinity and decreasing humidity conditions can reduce WUE within plants. Only the most saline tolerant species with the highest overall WUE (but low rates of C assimilation) may remain unimpacted by changes to salinity [*Ball et al*., 1988]. In the Everglades of Florida, United States, it has been shown that salinities equal to or exceeding that of seawater (35 parts per thousand, ppt) and high net radiation ($R_{net} > 500$ W m^{-2}) lead to reduced stomatal conductance and carbon assimilation rates, implying that such variables must be considered in ecophysiological models used in mangrove systems [*Barr et al.,* 2009].

At the ecosystem level, there is a dearth of information about the responses of mangrove forests to the elevated available energy in tropical environments or to the elevated evaporative demand that can be imposed by atmospheric conditions. The ecophysiological responses of mangrove ecosystems are also affected by other regional and global controls such as inundation levels (i.e., water management and storms), soil-pore water salinity, nutrients, tropical storms, cold air masses, air warming, and sea level rise. The first objective of this study was to identify and quantify meteorological and biophysical controls on diurnal and seasonal rates of water vapor fluxes for mangrove forests in the western Everglades of Florida. The second objective was to modify and verify the fidelity of existing evapotranspiration models to reproduce eddy covariance (EC)-derived daily and seasonal rates of water vapor exchange in these mangrove forests. Such models hold promise for improving water budgets and hydrologic modeling along the coasts of south Florida.

2. Methods

2.1. Mangrove Study Site

To investigate water vapor fluxes and associated meteorological and biophysical variables in mangrove forests, we instrumented a 28 m tower at the mouth of the Shark River in Everglades National Park. The tower became operational on 6 January 2004. The flux tower site is part of the Ameriflux network (US-Srk). Water fluxes were estimated using the EC approach, which entails an open path carbon dioxide (CO_2) and water vapor gas analyzer (Model LI-7500, LI-COR, Inc., Lincoln, NB) and a 3-D sonic anemometer (Model RS-50, Gill Co., Lymington, England). Continuous measurements at the site were used to determine the surface energy balance. Specific conductivity and temperature (Model 600R water quality sampling sonde, YSI Inc., Yellow Springs, Ohio) and water level (Model Waterlog H-333 shaft encoder, Design Analysis Associates, Logan, Utah) were continuously measured in a shallow well at an adjacent site located ~100 m from the tower. Salinity was determined from a known function of conductivity and water temperature. Meteorological variables were averaged over 30 min intervals to investigate diurnal relationships and were presented as daily sums to identify seasonal trends (using gap-filled data [*Barr et al.,* 2010]).

The plant canopy at the study site is dominated by red (*Rhizophora mangle*; dominant spp.), black (*Avicennia germinans*), and white (*Languncularia lacemosa*) mangroves. The forest canopy is approximately 15–20 m high, with a leaf area index of about 3 m^2 m^{-2}. The site experiences semidiurnal tides, with two high tides per day on most days. Maximum tides reach approximately 0.5 m. Annual rainfall typically exceeds 1500 mm with 60% occurring during May to October in the Everglades [*Duever et al.*, 1994]. Salinity fluctuates seasonally from approximately 10–15 ppt during October–November to 35–40 ppt during May–June.

2.2. Surface Energy Balance

We used surface energy flux data to identify diurnal and seasonal patterns in water vapor fluxes. The surface energy balance is defined as

$$R_{net} - G - \Delta H_{tot} - S = LE + H \quad (1)$$

where R_{net} is net radiation, G is thermal conduction into the soil (i.e., soil heat flux), ΔH_{tot} is thermal energy transferred into the water column [*Barr et al.*, 2013a, 2013b], and S is energy required to heat (or cool) aboveground biomass between the surface and eddy covariance height as well as chemical energy stored during photosynthesis [*Gu et al.*, 2007]. A net radiometer (model CNR1, Kipp and Zonen, Delft, Netherlands) deployed at 30 m above the ground recorded R_{net}. Available energy is partitioned into sensible (H) and latent (LE) heat fluxes, which were determined as 30 min averages from 10 Hz eddy covariance measurements [*Barr et al.,* 2010]. Heat flux plates (model HFP01, Campbell Scientific Inc., Logan, UT) placed at a depth of 5 cm in

the soil recorded G. We did not make the necessary measurements for estimating S or ΔH_{tot} for the mangrove forest, and therefore, the amount of energy available for transfer to the atmosphere (i.e., available energy) was simplified to $R_{net} - G$.

During 2004 to 2009, the mangrove forest energy balance at this site was closed within 70–80% [*Barr et al.*, 2012] when S and ΔH_{tot} were not included. Including S and ΔH_{tot} can improve closure of the surface energy budget by as much as 10% [*Gu et al.*, 2007] for most forests and 5% for mangrove forests [*Barr et al.*, 2013a, 2013b], respectively. To evaluate the relative strengths of the sensible and latent heat fluxes throughout the study period, we calculated the Bowen ratio ($\beta = H/LE$). In deserts, where radiational loads are high and little water is available to evaporate or transpire, β can exceed 10. Over tropical oceans and in forests where water is abundant, β values are typically less than 0.5. To compare the magnitude of water vapor fluxes relative to other observed and modeled values, we also corrected the observed latent heat flux (LE_c) to account for the lack of closure in the energy balance using the Bowen ratio method [*Twine et al.,* 2000],

$$LE_c = \frac{R_{net} - G}{1 + \beta} \tag{2}$$

This method can result in LE_c values exceeding the EC-derived LE by 10–30% during midday when closure of the surface energy budget is the lowest (75–90%). Values of LE_c were chosen for further analysis over EC-derived LE. LE_c may include a slight positive bias (~5%) since S and ΔH_{tot} were ignored, but EC-derived LE likely exhibits an average negative bias of 20 to 30% based on the energy balance considerations.

2.3. Meteorological, Hydrological, and Biophysical Controls on Evapotranspiration

Salinity was investigated as a potential control on daily sums of LE_c. We hypothesized that increased salinity would result in decreased rates of transpiration of individual mangrove trees coincident with increased osmotic potentials across root-surface interfaces. Lowered transpiration would be evident in lowered daily LE_c. To test this hypothesis, daytime sums of LE_c were scaled by daytime sums of available energy (i.e., $\sum LE_c/\sum(R_{net} - G)$), and these ratios were linearly regressed against daily average salinity values. Rejection of the null hypothesis (that salinity has no effect on latent heat fluxes) required that the slope of the least-squares (LS) regression line had a slope < 0 with 95% confidence ($P < 0.05$). The effect of VPD was also analyzed within this framework by partitioning data into three equally sized bins sorted by daytime average VPD. Ratios were regressed against salinity for each of these three data sets. We expected the control of salinity on the partitioning of LE_c to be more pronounced during those days with higher average VPD when the demand for water vapor transport was larger.

Meteorological drivers and biophysical controls dictate the magnitude of the flux of water vapor from a plant canopy. Vapor pressure deficit and net radiation are the primary meteorological drivers, whereas the canopy conductance to water vapor accounts for the role of plant physiology in determining the latent heat flux. This canopy conductance (g_{cv}, in m s^{-1}) is the inverse of the canopy resistance (r_{cv}), which can be estimated using EC measurements based on the Penman-Monteith relationship [*Monteith and Unsworth*, 2013],

$$LE_c = \left[\Delta(R_{net} - G) + \rho_a C_p VPD g_{av}\right] / \left[\Delta + \gamma(1 + g_{av}/g_{cv})\right] \tag{3}$$

where ρ_a is the density of air (in kg m^{-3}), c_p is the specific heat of dry air (1005.7 J kg^{-1} K^{-1}), and γ is the psychrometric constant (0.067 kPa K^{-1}). The vapor pressure deficit (*VPD*) is determined as ($e_s - e_a$, in kPa) where e_a and e_s (in kPa) are the actual and saturation vapor pressure at the 27 m air temperature (T_a, in °C). The e_s was computed using Tetens equation ($e_s(T_a) = 0.611 \exp[17.27T_a/(T_a + 237.3)]$, and Δ (in kPa K^{-1}) is the slope of e_s with respect to T_a (i.e., $\Delta = 4098\, e_s(T_a)/(T_a + 237.3)^2$) [*Tetens,* 1930; *Murray*, 1967]. The g_{av} (in m s^{-1}) is the atmospheric conductance to water vapor transfer, where $1/g_{av}$ is given by $1/g_{am} + 1/g_{bv}$. The g_{am} (in m s^{-1}) is the aerodynamic conductance to momentum, and g_{bv} (in m s^{-1}) is boundary layer conductance to water vapor given as

$$g_{am} = k\, u_* / \ln\left(\frac{z_R - d_0}{z_{0m}} - \Psi_m\left(\frac{z_R - d_0}{L}\right)\right) \tag{4}$$

$$g_{bv} = (k\, u_*/2)\, (D_v/D_H)^{2/3} \tag{5}$$

where z_R is the reference height (27 m), d_0 is the canopy zero plane displacement (0.65h; h is the canopy height, 20 m), and z_{0m} is the roughness length for momentum sink (0.13h). Values of d_0 and z_{0m} were selected

Table 1. Least-Squares Regression Slope, Intercept, Explained Variance (R^2), and Significance of the Linear Relationship (P Value) of the Ratio of Daily Observed Latent Heat Flux (LE_c) to Net Radiation (R_{net}) Minus Soil Heat Flux (G) (i.e., Scaled Latent Heat Flux: $LE_c/(R_{net} - G)$) Versus Mean Surface Water Salinity During 2004 and 2005[a]

VPD Category	VPD Range (kPa)	Slope (ppt^{-1}) (Mean ± 95% CI)	Intercept (Unitless) (Mean ± 95% C.I.)	R^2	P Value
All data	0.16 to 2.23	−0.0111 ± 0.0025	0.891 ± 0.069	0.138	< 0.01
Low	0.16 to 1.16	−0.0089 ± 0.013	0.794 ± 0.351	0.045	0.01
Mid	1.16 to 1.48	−0.016 ± 0.009	1.029 ± 0.242	0.248	< 0.01
High	1.48 to 2.23	−0.012 ± 0.005	0.946 ± 0.132	0.383	< 0.01

[a]Regressions were performed using all the data and separately where data were ranked by daily mean vapor pressure deficit (VPD) and sorted into tertiles (low, mid, high).

in modeling studies [*Barr et al.*, 2009] of CO_2, water vapor, and sensible heat fluxes at this site and are within the range of those reported [*Arya*, 1988] for vegetated canopies. The Ψ_m is the integral form of the diabatic correction function for mass transfer and provides an adjustment to the logarithmic wind profile during nonneutral (statically stable or unstable) atmospheric conditions. The L is the Obukov length (in m), k is von Karman's constant ($k = 0.4$), and u^* is friction velocity (in m s^{-1}). The D_H and D_v are the thermal diffusivity and molecular diffusivity for water vapor, respectively, and the ratio D_v/D_H is 1.121 at air temperature of 298 K.

Several quantities were derived to understand seasonal and diurnal patterns in the controls on latent heat fluxes. Equilibrium (LE_{eq}) and imposed (LE_{imp}) latent heat exchange (in W m^{-2}) include the meteorological and physiological controls on LE_c, respectively, and are given by

$$LE_{eq} = \frac{\Delta}{(\Delta + \gamma)}(R_{net} - G) \tag{6}$$

$$LE_{imp} = \rho_a C_p g_{cv} VPD/\gamma \tag{7}$$

Together, LE_{eq} and LE_{imp} represent two boundary conditions for latent heat exchange. A linear scaling, termed the canopy decoupling coefficient Ω [*McNaughton and Jarvis*, 1991; *Jarvis and McNaughton,* 1986], was defined to describe the relative importance of atmospheric versus vegetation controls and may be described in terms of LE_c or Ω as follows:

$$LE_c = \Omega LE_{eq} + (1 - \Omega)\, LE_{imp} \tag{8}$$

$$\Omega = \left(LE_c - LE_{imp}\right)/\left(LE_{eq} - LE_{imp}\right) \tag{9}$$

The Ω was also calculated [*Jarvis and McNaughton*, 1986; *Kumagai et al.*, 2004] as

$$\Omega = \frac{\Delta/\gamma + 1}{\Delta/\gamma + 1 + g_{av}/g_{cv}} \tag{10}$$

where all terms were defined previously. Its range is 0 to 1; when $\Omega = 1$ there is perfect coupling ($LE_c \rightarrow LE_{imp}$); when $\Omega = 0$ there is perfect decoupling ($LE_c \rightarrow LE_{eq}$) with the atmosphere, respectively. Besides 30 min average values, daily average Ω were also computed using two different approaches. The LE_c, LE_{eq}, and LE_{imp} were summed during daytime periods, and daily Ω (Ω_{day}) values were determined according to equation (9). Also, the Ω values were determined for each 30 min period during the daytime and a weighted average was computed as

$$\Omega_{day} = \sum(LE_c \times \Omega)\Big/\sum LE_c \tag{11}$$

2.4. Modeling Evapotranspiration

To evaluate whether water vapor flux models may be applied to mangrove forests, we tested both a modified version of the Penman-Monteith (PM) model [*Monteith and Unsworth*, 2013] and Priestley-Taylor (PT) [*Priestley*

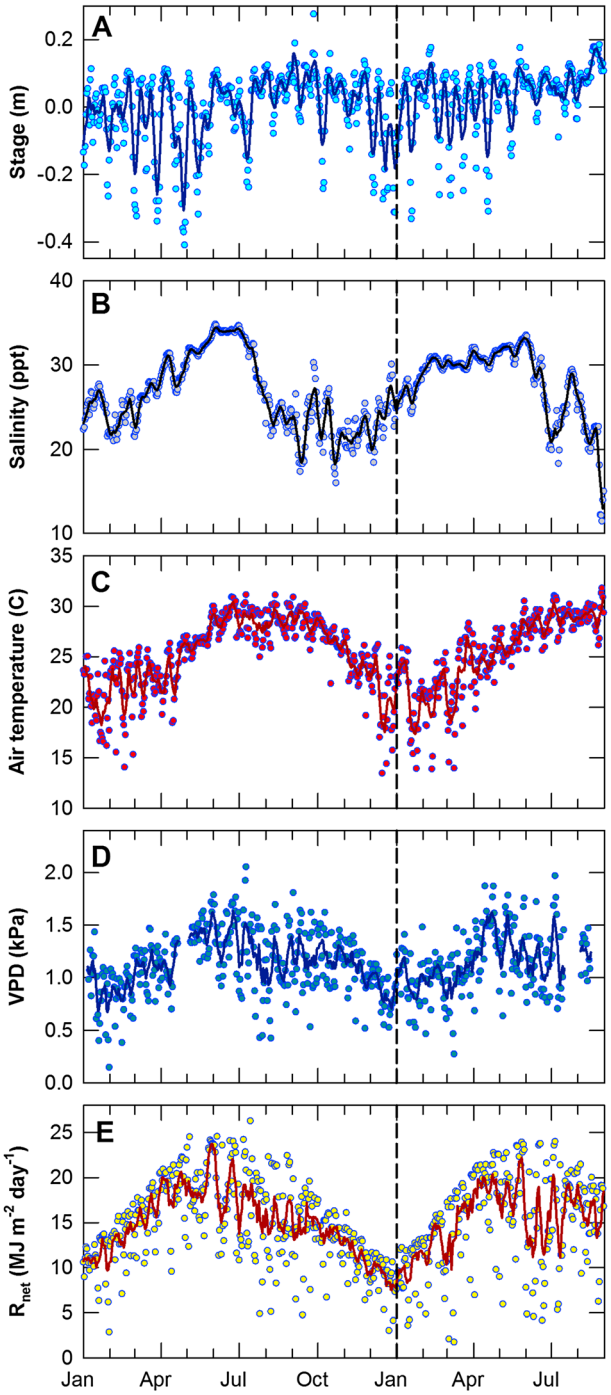

Figure 1. Seasonal patterns in daily environmental variables and 7 day moving averages during 2004 and 2005. Variables include (a) daily average stage in meter, (b) average salinity in parts per thousand, (c) average air temperature in degree Celsius at 27 m, (d) average vapor pressure deficit at 27 m in kPa, and (e) daytime sums of net radiation above the canopy at 27 m in MJ m^{-2} d^{-1}.

and Taylor, 1972] model. The Penman-Monteith model was implemented by estimating g_{cv} during the daytime from inversion of equation (3) as

$$\frac{1}{g_{cv}} = r_{cv} = \left(\Delta \frac{1}{g_{aH}} (R_{net} - G) + \rho_a \; C_p \; D\right) \Big/ (\gamma \; LE_c) - \left(\frac{\Delta}{\gamma}\right) \frac{1}{g_{aH}} - \frac{1}{g_{av}} \tag{12}$$

where g_{aH} is the atmospheric conductance to heat transfer (in m s^{-1}) and $g_{aH} \sim g_{av}$ was assumed from similarity theory. The g_{cv} values were then modeled in two different ways and substituted into equation (3) to

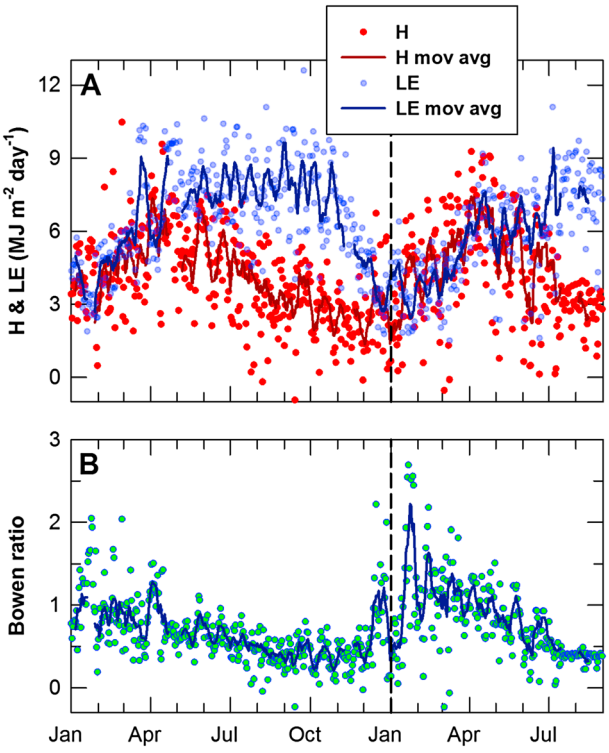

Figure 2. (a) Daily (daytime) sums of sensible (*H*) and latent (*LE*) heat exchange and (b) 7 day moving averages during 2004 and 2005 along with Bowen ratios computed as *H*/*LE*.

derive a Penman-Monteith estimate for the latent heat flux. First, a baseline model (PM ver1) was formulated using a constant g_{cv} set equal to the median g_{cv} of all daytime periods during 2004 and 2005. This g_{cv} was the single value best estimate representative of the entire study period. Second, g_{cv} was modeled using multiple least-squares (LS) linear regression (PM ver2). Potential explanatory variables were selected and included daily daytime averages (weighted by 30 min $R_{net} - G$) of salinity, air temperature, VPD, solar irradiance, and friction velocity. Multiple LS-regression was selected as the model structure for two reasons which are (1) seasonal patterns of g_{cv} appeared to covary linearly with multiple environmental drivers, including salinity, air temperature, and VPD, and (2) a simple linear model accommodates explanatory variables not included in existing models of g_{cv}. For instance, the Lohammar equation [*Lundblad and Lindroth*, 2002] assumes that g_{cv} declines hyperbolically with VPD, but our model must be flexible to include other factors known to influence seasonal patterns in surface exchanges of CO_2 and water vapor. Next, 30 min estimates of g_{cv} were computed from the linear model using LS-regression coefficients, and LE estimates were determined from substitution of g_{cv} into (3). The Priestley-Taylor (PT) model was also assessed for its ability to reproduce seasonally varying rates of LE and is given by

$$LE_{PT} = \alpha \; LE_{eq} \tag{13}$$

where α is the PT coefficient. This formulation (13) is equivalent to assigning the aerodynamic term of the Penman equation to be a constant fraction of net radiation (J. Jacobs et al., Satellite-based solar radiation, net radiation, and potential and reference evapotranspiration estimates over Florida, USGS Technical Report submitted to the *USGS*, http://hdwp.er.usgs.gove/ET/GOES_FinalReport.pdf, 2008) and serves as a way to compare observed ET to that expected over a "wet" surface assuming a closed volume and constant net radiation [*McNaughton and Jarvis*, 1983; *Wilson and Baldocchi*, 2000]. It has been suggested that α converges to a limiting value of 1.26 [*Priestley and Taylor*, 1972] or to a range between 1.1 and 1.4 [*Monteith*, 1995] with increasing g_{cv}. However, there is no theoretical basis for expecting α to converge to a theoretical limit [*Wilson and Baldocchi*, 2000]. In this study, daily values of α were computed as $\sum LE/\sum LE_{eq}$ and daily g_{cv} as daytime averages weighted by 30 min ($R_{net} - G$). Daily α was modeled as a power function of g_{cv} as

$$\alpha_{model} = p_1 {g_{cv}}^{p_2} \tag{14}$$

where p_1 and p_2 are coefficients determined from nonlinear regression. Use of a power function was similar to the approach of *Ryu et al.* [2008], who fit α to a logarithmic function of g_{sv}. However, the power function compared to a logarithm provided additional flexibility in the shape of the α versus g_{cv} response curve. Daily *LE* were then modeled from (13) using both median of daily α during the study period (PT ver1) and using the power function estimate of α (PT ver2) in (14) using g_{cv} determined from multiple linear regression (see PM ver2). Direct estimates of g_{cv} (12) could not be used since these values are computed using observed LE_c. The root-mean-square error (RMSE) and bias error were determined for daily evapotranspiration, *ET*, calculated from all of the PT and PM models as compared to the measurements, i.e., *ET* (in mm day^{-1}) = 0.4095 × *LE* (in MJ m^{-2} day^{-1}), during 2004 and 2005 (Table 1).

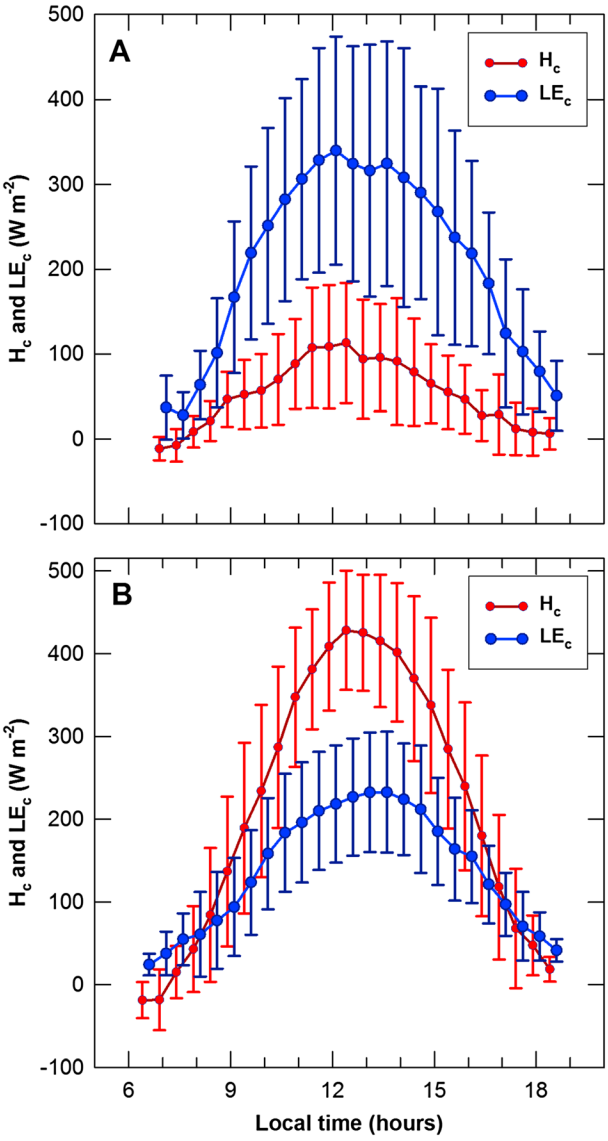

Figure 3. Diurnal patterns (period average ± 1 s.d.) in energy balance corrected sensible (H_c) and latent (LE_c) heat fluxes segregated into periods representing the (a) lowest and (b) highest 10% of daily average Bowen ratios during 2004 and 2005 (Figure 2b).

3. Results

3.1. Meteorological, Hydrological, and Biophysical Controls on Evapotranspiration

Levels of inundation and surface water salinity exerted influence on the evapotranspiration of the mangrove forest. Daily median water levels were most consistently high (frequently exceeding 0.0 m) during the end of the wet season in October–November (Figure 1a) when water levels were highest upstream in the fresh water marshes. These periods coincided with seasonally maximal freshwater flows toward the Gulf of Mexico and with seasonally minimal salinity levels ($<$ 25 ppt, Figure 1b). During the dry season months of January to May, average water levels often dropped below -0.1 m, and the normal semidiurnal pattern of inundation ceased for several days in succession. Such patterns were the result of reduced freshwater flows through Shark River and the influence of northerly winds, which prevent high tides in the Gulf of Mexico from propagating inland into the estuary. During these dry season months, there was an increasing trend in salinity values, from average daily values of as low as 20 ppt in January toward peak average values of about 35 ppt by July and August.

Seasonal air temperature variability dictated atmospheric saturation vapor pressure which in turn influenced evaporative demand. Air temperatures at 27 m were highest ($>$ 25°C, Figure 1c) during May to September, coincident with the early to middle wet season. Therefore, moving averages of seasonal VPD values were also higher during this period (commonly reaching at least 1.5 kPa, Figure 1d). However, daily VPD was $<$1 kPa during days with overcast or mostly cloudy conditions when relative humidity (not shown) exceeded 80%. Daily sums of net radiation (Figure 1e) were most consistently high during May (averaging approximately 20 MJ m^{-2} day^{-1}), just prior to the onset of the wet season. The temporal trend in R_{net} was more variable during June to October; while many days had values exceeding 20 MJ m^{-2} day^{-1}, frequent cloudy days regularly lowered the moving average relative to trends observed in May. Lowest R_{net} (around 10 MJ m^{-2} day^{-1}) occurred during December and January coincident with the winter solstice.

3.2. Controls on the Surface Energy Balance

Daily sums of H and LE were nearly equivalent throughout December to April, leading to relatively high Bowen ratios of around, but frequently exceeding, 1.0 (Figure 2). Particularly during the dry season months of January to March, more available energy was often partitioned as H than LE (i.e., $\beta > 1$), a feature commonly observed in semiarid environments [*Heusinkveld et al.,* 2004]. During these months, soil and air temperatures were seasonally lowest (with daily averages of 15–23°C and 14–26°C, respectively)

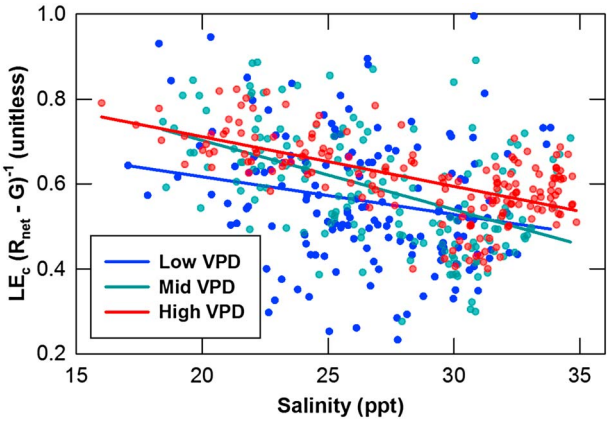

Figure 4. Daily ratios of daytime sums of energy balance adjusted latent heat flux (LE_c) to available energy ($R_{net} - G$) versus daily average salinity during 2004 and 2005. Data were partitioned equally into three bins (i.e., low, mid, and high) by average daytime vapor pressure deficit, and LS-regression was performed for each binned data set. The mid and high VPD bins had significant correlations (see Table 1).

and daily average VPD tended to be low (< 1.0 kPa) (Figure 1d). Both *H* and *LE* fluxes increased during this period, from approximately 3 MJ m^{-2} day^{-1} to over 6 MJ m^{-2} day^{-1}. During February to June, increasing salinity levels partially mitigated the rate of increase in *LE* in response to increasing daytime air temperatures and VPD (from 15 to 32°C and from 0.5 to 2.8 kPa, respectively). During these months, seasonally lower evaporative demand combined with lower physiological activity, when average daily air temperatures were below 20°C, resulted in seasonally low transpiration rates. Also, soil temperatures at 5 cm depth were 3.0–3.5°C lower than air temperatures at 27 m [see *Barr et al.,* 2012, Table 1], likely due to cool (20–25°C) waters that flooded the surface nearly twice daily, and likely contributed to lowered surface evaporation rates. Negative lapse rates between heights of 1.5 and 20 m of -47 ± 30 °C km^{-1} (daytime average ± 1 standard deviation during January to May 2004) [see *Barr et al.,* 2012, Table 1] suppressed the turbulent exchange of humid air below the forest canopy with the overlying air mass, further inhibiting surface evaporation.

During the wet season, salinity declined rapidly from about 35 ppt in June and July to between 17 ppt and 26 ppt in August. These declines in salinity, combined with sustained air temperatures of 28–32°C and midday VPD of 1.5–3.0 kPa, resulted in partitioning of larger fractions of R_{net} into *LE* and subsequently smaller fractions as *H,* lowering daily Bowen ratios (to 0.5–1.0, Figure 2b). Thus, in contrast to the dry season, the mangrove forests behaved more like broadleaved tropical forests during wet season months of June to November with β commonly at or below 0.5 (Figure 2b). Seasonal differences in energy partitioning patterns were also apparent in diurnal profiles of H_c and LE_c representing days with the lowest (Figure 3a) and highest (Figure 3b) 10% of daily average Bowen ratio (Figure 2b). During days with a low Bowen ratio (Figure 3a), midday LE_c exceeded H_c by a factor of 3. During days with a high Bowen ratio (Figure 3b), H_c and LE_c were nearly equal during early morning (7:00 to 9:00 hours) and late afternoon (16:00 to 19:00 h), but H_c was double that of LE_c during the middle of the day (11:00 to 14:00 hours). During midday, a thermal inversion formed between the canopy crown and the cool surface. Such stable conditions tended to suppress atmospheric mixing and reduced surface evaporation. In the cooler dry season months, statically stable conditions below the canopy became common as a result of warming air masses during the day and maintenance of a lower temperature surface from inundation by cool waters from the Gulf of Mexico during high tides. The energy partitioning that resulted in high Bowen ratio values (> 1.0) occurred during December to April.

Energy budget adjusted latent heat fluxes as a fraction of daily available energy (i.e., scaled LE_c; LE_c $(R_{net} - G)^{-1}$) declined substantially (Table 1) with increasing salinity (Figure 4) during the study period. Much of the scatter in the data occurred during days having the lowest tertile of average daily VPD (Figure 4; low VPD, $R^2 = 0.05$) when air temperatures were lowest (< 20°C) and during cloudy days when available energy was reduced (<10 MJ m^{-2} day^{-1}). During these low VPD periods, the change in scaled LE_c with salinity was negative and significant but the slope of the regression line was variable (Table 1). During all other periods when VPD was higher (upper two tertiles of VPD), significance values of the regression line were higher ($P < 0.01$) and confidence intervals of the slope were tighter (Table 1) compared to those of the lowest tertile of VPD. Results indicated that salinity also partially controlled evapotranspiration through physiological controls on transpiration. As salinity increases, the osmotic potential between pore water and roots increases and the energetic cost of transpiring water increases; thus, under these conditions, mangrove trees likely partially close leaf stomata to reduce transpiration [*Barr et al.,* 2009]. However, quantifying any reduction in

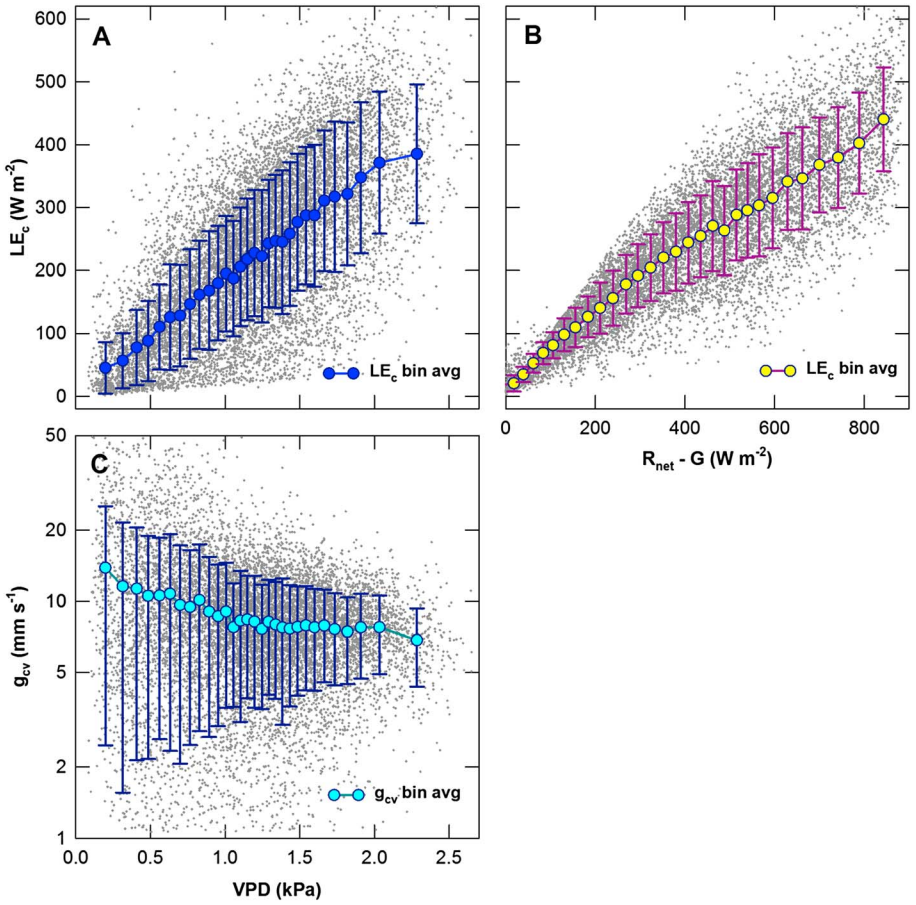

Figure 5. Energy balance corrected 30 min average latent heat fluxes (LE_c) response (a) to vapor pressure deficit (VPD) and (b) to available energy ($R_{net} - G$) and (c) response of canopy conductance to water vapor (g_{cv}) to VPD during 2004 and 2005. The scale for g_{cv} (Figure 5c) is logarithmic. The 30 min data were partitioned equally into 30 bins along the abscissa and averaged. Error bars represent ± 1 s.d. around the mean.

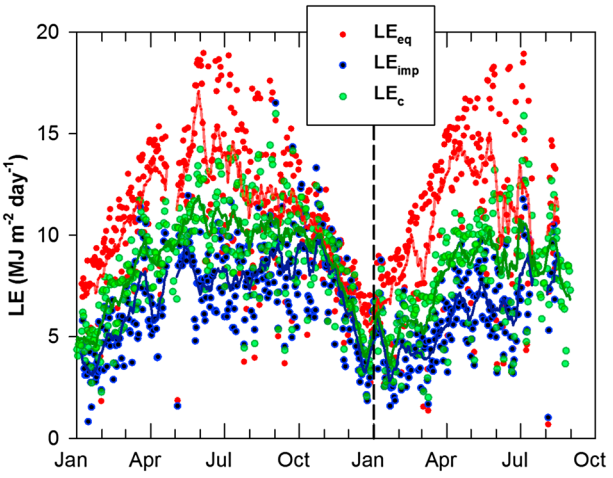

Figure 6. Daily sums of equilibrium (LE_{eq}), imposed (LE_{imp}), and energy balance corrected latent heat flux (LE_c) during 2004 and 2005. Only daytime periods were included in daily sums, and lines represent 14 day moving averages of daily values.

transpiration and changes in energy partitioning within the canopy may be difficult during periods when evaporative demand is low (< 1 kPa) since the fractional contribution of surface evaporation to evapotranspiration is generally large and variable under these conditions. As a consequence of partially closed stomata and conservative use of water, mangrove trees pay a price of reduced net ecosystem exchange of carbon (NEE) [*Barr et al.,* 2010] and lowered gross primary productivity (GPP) [*Barr et al.*, 2013a, 2013b].

3.3. Meteorological Drivers and Biophysical Controls on Evapotranspiration

Availability of energy and VPD were primary drivers of the magnitude of LE_c (Figures 5a

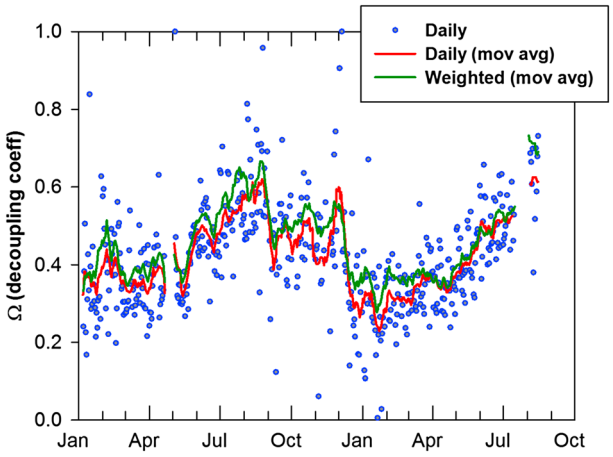

Figure 7. Daily average decoupling coefficients (Ω) during 2004 and 2005. The Ω values were determined as a ratio of daily sums of ($LE_c - LE_{imp}$) to ($LE_{eq} - LE_{imp}$) (i.e., daily Ω) and as averages of 30 min Ω (equation (10)) weighted by LE_c. For clarity, only the moving average of weighted Ω is shown. The LE_{eq}, LE_{imp}, and LE_c are equilibrium, imposed, and energy balance corrected latent heat fluxes, respectively.

and 5b, respectively). The observed considerable variance of LE_c with VPD may be partially attributed to periods of relatively high VPD (0.5 to 2.0 kPa) when the amount of available energy ($R_{net} - G$) was insufficient to support evapotranspiration. Such condition was evidenced in comparing the overall correlation ($R^2 = 0.64$) between VPD and available energy with that ($R^2 = 0.36$) of the subset of data restricted to available energy < 300 W m^{-2}. While LE_c generally increased with increasing VPD and available energy, canopy conductance to water vapor, g_{cv}, asymptotically declined with increasing VPD (Figure 5c). However, the trend is nearly linear for VPD > 0.5 kPa. These patterns suggest that water loss through transpiration is limited by the soil and root system. With increasing VPD and available energy during midday, physiological controls result in partial stomatal closure to ameliorate water loss through transpiration and to maintain favorable water potential in individual trees.

The imposed evaporative demand and the equilibrium rate of evapotranspiration represented two key boundary conditions useful for understanding observed patterns in daily latent heat fluxes (Figure 6). Daily LE_{eq} depended strongly on net radiation and therefore seasonal patterns closely followed available energy (Figure 1e). Maximum LE_{eq} values reached nearly 20 MJ m^{-2} day^{-1} in May and June, declined and became more variable during the wet season in June to October, and fell to minimum values (< 10 MJ m^{-2} day^{-1}) during the winter solstice in late December. The imposed equilibrium depends on both atmospheric and physiological variables and the moving average remained nearly constant from May to November ($LE_{imp} = 5$–10 MJ m^{-2} day^{-1}; Figure 5) in response to broad wet season maxima of near optimal air temperature (25–30°C; Figure 1c), relatively stable VPD (1.0–1.5 kPa; Figure 1d), seasonal maxima in g_{cv} (not shown), and declining salinity levels. Two week moving averages of LE_c were about 0 to 3 MJ m^{-2} day^{-1} higher than LE_{imp} but generally followed the seasonal pattern of LE_{imp} (Figure 6). The LE_{eq} was greater than LE_c, and this difference was most pronounced during February to May. During October and November, LE_{eq} declined and nearly converged with LE_{imp}. Consequently, LE_c was less sensitive to the relative controls of imposed and equilibrium processes on latent heat fluxes during this time period.

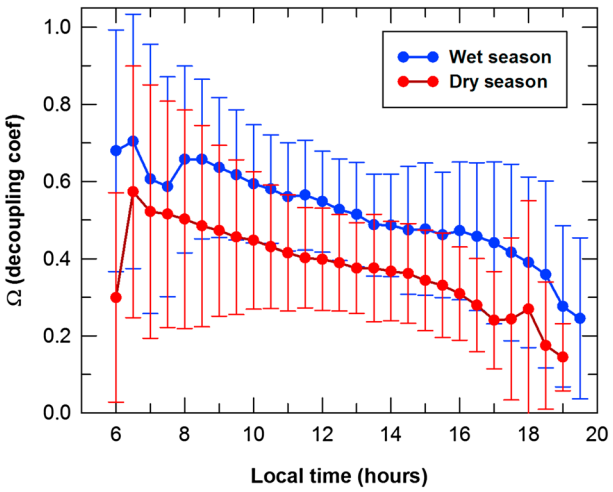

Figure 8. Diurnal averages ± 1 standard deviation of the decoupling coefficient (Ω) during 2004 and 2005 partitioned into wet (June to October) and dry (November to May) season periods.

The controls on latent heating were more clearly identified by seasonal trends in the decoupling coefficient, Ω (Figure 7). For estimates of daily Ω (the ratio of LE sums and weighted 30 min averages), the coupling of mangrove forest water vapor exchange to the atmosphere was greatest during December to April (Ω = 0.2–0.5, i.e., period of low decoupling with the atmosphere, when $LE_c \rightarrow LE_{eq}$). These trends in Ω were likely the result of reduced physiological activity and

Table 2. Parameters (Mean ± 95% CI) Determined From Multiple Linear Regression ($R^2 = 0.386$) of Daily Average Canopy Conductance to Water Vapor (g_{cv}) Weighted by Available Energy (Net Radiation (R_{net}) − Soil Heat Flux (G)) During 2004 and 2005[b]

Forcing Term	Regression coefficient (Mean ± 95% CI)	Range of Forcing	Relative Importance[a] (mm s^{-1})
Intercept (m s^{-1})	$1.22 \pm 0.227 \times 10^{-2}$	NA	NA
Salinity (ppt)	$-2.34 \pm 0.50 \times 10^{-4}$	18.0	−4.22
Solar irradiance (W m^{-2})	$-7.27 \pm 1.89 \times 10^{-6}$	835	−6.07
VPD (kPa)	$-1.12 \pm 0.99 \times 10^{-3}$	2.0	−2.28
Air temperature (°C)	$3.10 \pm 0.72 \times 10^{-4}$	18.0	5.57
Friction velocity (m s^{-1})	$2.99 \pm 1.23 \times 10^{-3}$	1.2	3.51

[a]Relative importance is defined as the product of the regression coefficient and the range of the forcing determined on a daily time step (i.e., Regression coefficient × Range of forcing).
[b]The canopy conductance values were used with Penman-Monteith model ver2 (see Table 3 and Figure 10).

therefore reduced stomatal opening during December to February and increased salinity during February to April. Also, water temperatures were seasonally lowest (< 25°C) during this period and lapse rates were usually negative (−47 ± 30 to −48 ± 44 °C km^{-1}; mean ± 1 standard deviation) [*Barr et al.,* 2012, Table 1] which likely contributed to reduced surface evaporation contribution to the latent heat flux. In contrast, during August and September, the mangrove forest reached minimal coupling to the atmosphere with moving average Ω values of 0.6–0.7 (i.e., high decoupling, when $LE_c \rightarrow LE_{imp}$). During this time, water and soil surface temperatures were seasonally highest (~30°C) which likely increased the proportion of surface evaporation to daily evapotranspitation. Throughout the study period, daily Ω seldom exceeded 0.75 suggesting that physiological controls and forest-atmospheric coupling at least partially controlled latent heat fluxes during the entire study period. These physiological controls were important even though the peat surface was perpetually wet and was inundated twice daily by high tides, except for a few isolated periods during the dry season.

The decoupling coefficient declined throughout the day, on average, during both dry and wet season periods (by about 0.4, Figure 8). This result indicated a process of increasing physiological controls on stomatal conductance and evapotranspiration during the afternoon, and this control persisted after solar noon when available energy was declining. During this time, mangrove trees may be conserving water and optimizing water use efficiency. Also, values of Ω were on average 0.1–0.2 higher during wet compared to dry season periods. These patterns likely resulted in response to increased physiological activity, decreased salinity, and higher average soil and water surface temperatures during the wet season. Such conditions promoted increased transpiration and surface evaporation.

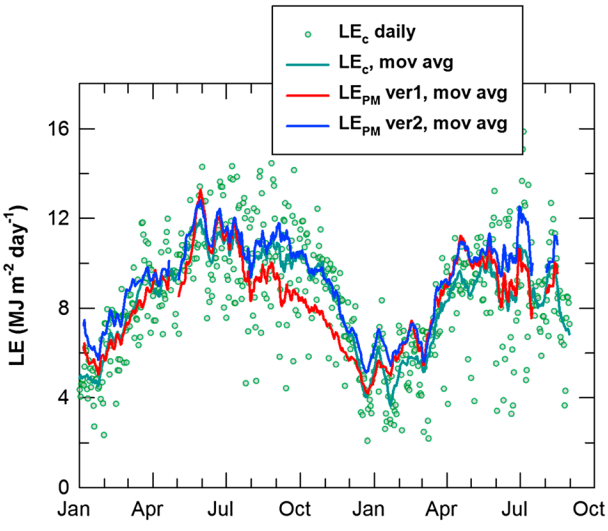

Figure 9. Daily sums of energy balance adjusted latent heat flux (LE_c) and 7 day centered moving average. Two variations on canopy conductance for water vapor (g_{cv}) were utilized in the Penman-Monteith model to estimate *LE*, shown as 7 day centered moving averages. Variations included a constant g_{cv} equal to the 30 min median during all of 2004 and 2005 (PM ver1), and g_{cv} modeled using multiple LS regression (PM ver2).

3.4. Reliability of Water Vapor Flux Models

Versions of Penman-Monteith and Priestley-Taylor models adequately reproduced daily and seasonal evapotranspiration rates estimated from eddy covariance. The simplest form of the Penman-Monteith model (PM ver1), which used a constant daytime median g_{cv} of 7.7 mm s^{-1}, under predicted daily rates of LE on average during August to November 2004. A single constant value for g_{cv} was therefore determined insufficient for modeling seasonal rates of ET. Instead, daily average canopy conductance was found to covary negatively with salinity,

Table 3. Cumulative Evapotranspiration (ET) Calculated From Observed Latent Heat Fluxes (LE_c) and Modeled During 2004 and 2005 (Through 31 August)[a]

Model	ET Totals (mm)		Bias Error (mm day^{-1})		RMSE, 2004–2005 (mm day^{-1})	R^2, 2004–2005
	2004	2005 Jan–Aug	2004	2005 Jan–Aug		
EC-LE_c	1320	779	NA	NA	NA	NA
PM ver1	1242	820	−0.062	0.068	0.570	0.876
PM ver2	1397	872	0.061	0.146	0.528	0.928
PT ver1	1291	847	−0.023	0.109	0.674	0.840
PT ver2	1306	825	−0.011	0.070	0.500	0.900

[a]Penman-Monteith (PM) models used a constant canopy conductance to water vapor (g_{cv}; PM ver1 (median of all daytime values during 2004 and 2005)), and modeled canopy conductance determined from multiple LS-regression (PM ver2). Priestley-Taylor (PT) models included the median of daily α during the 2004–2005 study period (PT ver1), and α modeled as a power function (equation (14)) of daily weighted g_{cv} (PT ver2). Error metrics include Bias Error (sums of daily (ET modeled − ET observed)) and root-mean-square error (RMSE) of daily ET (where error is ET modeled − ET observed).

solar irradiance, and VPD and positively with increasing air temperature and surface friction velocity (Table 2). These multiple LS-regression coefficients help explain why using a single value of g_{cv} resulted in under predicting daily LE during August to November 2004. Near optimal physiological activity along with seasonally decreasing salinity, midday VPD, and midday solar irradiance all contributed to higher modeled g_{cv} (see Table 2) and therefore higher *LE*. Though the ability of the multiple LS-regression model to predict daily g_{cv} was modest ($R^2 = 0.386$), modeled *LE* (PM ver2; Figure 9) exhibited little bias in comparing moving averages of LE_c and modeled *LE* (PM ver2). In addition, using variable compared to constant g_{cv} resulted in reduced root mean squared error (RMSE) and improved correlation (R^2; Table 3) during the 2004 to 2005 study period. The regression coefficients determined here (PM ver2) may be site specific, and this study needs to be replicated in other mangrove forests to learn if forcings are similar. Also, the magnitude of g_{cv} likely varies with the structure of mangrove forests and relative partitioning between transpiration and evaporation from the surface.

The daily Priestley-Taylor (PT) coefficient, α, varied monotonically with increasing g_{cv} (Figure 10) across the entire observed range of g_{cv} and necessitated a seasonally varying α. The best fit power function (14) suggested that α did not saturate at the highest observed daily g_{cv} (Figure 10). Results were in agreement with annual patterns reported by *Ryu et al.* [2008] over a grassland in California but were in contrast to earlier data sets [*Monteith*, 1995] where α approaches a limit (1.1 to 1.4) with increasing g_{cv}. Similar to the PM analysis where g_{cv} was held constant (PM ver1; Figure 9), selecting a constant value of α in evaluating (13) also resulted in under predicting daily LE during August to November 2004 (PT ver1; Figure 11). By using modeled g_{cv} and substituting into (13) to predict α, most of the seasonal biases were eliminated in comparing moving averages of modeled (PT ver2) to observed *LE*. Also, overall model performance (PT ver2) was comparable to Penman-Monteith derived estimates of *LE* using variable g_{cv} (PM ver2; Table 3). As with the Penman-Monteith models of g_{cv}, the Priestley-Taylor model parameterization of α is site-specific, and analyses need to be repeated to learn more general trends and patterns of α versus g_{cv} in mangrove forests.

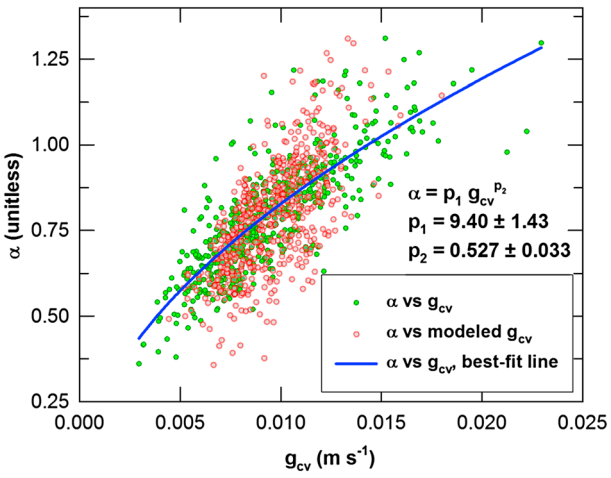

Figure 10. Relationship between daily weighted average Priestley-Taylor coefficient (α) and daily weighted average canopy conductance (g_{cv} (12)) and modeled g_{cv} determined from multiple linear regression. The line represents the best fit nonlinear regression of a power function (14) of α and g_{cv}. Coefficients p_1 and p_2 (mean ± 95% CI) were determined to be 9.40 ± 1.43 and 0.527 ± 0.033, respectively.

These Penman-Monteith and Priestley-Taylor models offered promise for modeling ET and understanding seasonally variable energy partitioning patterns in a mangrove forest. While general seasonal trends in daily ET can be represented by using a single

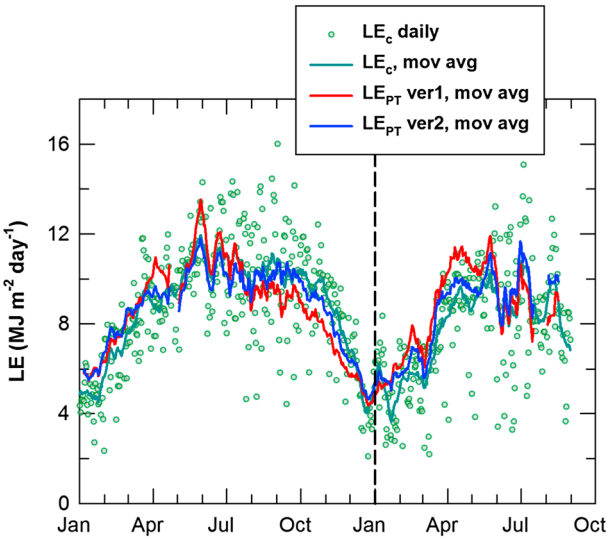

Figure 11. Daily sums of energy balance adjusted latent heat flux (LE_c) and 7 day centered moving average. Daily sums of *LE* calculated from two versions of the Priestley-Taylor (PT) model are also shown as 7 day centered moving averages: (PT ver1) the median of all daily α and (PT ver2) α determined from the best fit function (14) of daily α versus daily canopy conductance determined from multiple LS regression.

constant value for either g_{cv} or α in the PM and PT formulations, respectively, these simple models result in seasonal biases in latent heat fluxes. A better understanding of energy partitioning was gained by considering the interactive forcings of salinity, solar irradiance, VPD, air temperature, and friction velocity on both g_{cv} and α and therefore daily ET. Future improvements in modeling daily ET in mangrove forests may require the inclusion of seasonally variable structural information (e.g., leaf area index), physiological attributes (e.g., leaf nitrogen content), and parameterizations based on known rates of surface evaporation and transpiration. This study represents one of the first attempts to model energy partitioning trends in a mangrove forest.

4. Conclusions

The mangrove forests in the Everglades National Park of Florida exhibited variable partitioning trends of available energy into sensible and latent heat fluxes in response to physiological traits of mangrove trees and imposed atmospheric evaporative demand. During December to April in 2004 to 2005, the partitioning of the available energy into sensible and latent heat often resulted in Bowen ratio values exceeding 1.0. These Bowen ratios are comparable to those found in semiarid environments, and such patterns are not typically expected in ecosystems with plentiful water. In contrast, during the July to November period these mangrove forests behaved like well-watered broadleaved deciduous forests with Bowen ratios generally < 0.5. Such patterns were the result of seasonally variable air temperatures, available energy, vapor pressure deficits, and salinity levels. While air temperatures, net radiation or available energy, and vapor pressure deficits have traditionally been incorporated into numerical models to estimate evapotranspiration, salinity levels have not. Our results show that increasing surface water salinity resulted in reduced energy partitioning to latent heat fluxes consistent with modeled reductions in canopy conductance. Not accounting for the effect of salinity on g_{cv} and latent heat exchange can result in model biases of ~1 mm d^{-1} in ET. The observed and modeled relationships between salinity and ET identified in this study are consistent with the expected effects of increasing pore water salinity, such as increasing negative osmotic potentials across root membranes, conservative use of water by individual trees, and reduced ecosystem-scale transpiration (and therefore reduced ET).

On average, a salinity increase from the lowest (11 ppt) to the highest (35 ppt) salinity observed during 2004 and 2005 would result in a 26% reduction in available energy partitioned as latent heat flux. Consistent with Bowen ratio patterns, daily decoupling coefficients also varied seasonally with the lowest values (0.2 to 0.4) observed during December to April and highest values (0.5 to 0.7) observed during August to November. Such patterns reinforce the conclusion drawn from Bowen ratios that the forest shifts from a water conservative semiarid ecosystem during December to April to that of a well-watered broadleaved deciduous forest during August to November. Once appropriately modified to consider the effects of seasonally variable salinity, solar irradiance, VPD, air temperature, and friction velocity on ecosystem ET, Penman-Monteith, and Priestley-Taylor models adequately reproduced daily rates of ET during 2004 and 2005.

These results and analyses suggest that parameterized Penman-Monteith and Priestley-Taylor models may have value for large-scale ET modeling of mangrove forests globally. An important next step in modeling ET will be to make these models more general to account for differences in forest structure, environmental forcings (e.g., differences in subtropical versus tropical forests), and duration and frequency of inundation. Such models may be improved by accounting for site differences in the relative contribution of transpiration and evaporation to ET. Field and modeling experiments that distinguish between transpiration and evaporation

will be needed to improve parameterizations of g_{cv} and α. In terms of environmental forcings, it is worth noting that the levels of salinity observed at this study site (11–35 ppt) are lower than those experienced in other mangrove forests. Thus, future work should explore these relationships in more saline environments. While the maximum levels of salinity observed in this study were roughly equal to seawater, other mangrove forests experience 2–3 times that amount [*Ball,* 1988]. Larger-scale studies are also needed to address the magnitude and ranges of canopy conductance and the Priestley-Taylor coefficient (α) and must identify a set of common forcings on either g_{cv} or α. The forcings identified here—salinity, solar irradiance, VPD, air temperature, and friction velocity (or wind speeds)—represent a good starting point for further investigation in mangrove forests globally.

Acknowledgments
The Jones Everglades Research Fund provided support to establish the flux tower and to instrument adjacent sites. The National Science Foundation provided support for this research (award WSC-0920504). Also, the National Science Foundation also supported this research through the Florida Coastal Everglades Long-Term Ecological Research (awards DBI-0620409 and DEB-9910514).

References

Arya, S. P. (1988), *Introduction to Micrometeorology*, edited by R. Dmowska and J. R. Holton, pp. 148–152, Academic Press, San Diego, Calif.
Ball, M. C. (1986), Photosynthesis in mangroves, *Wetlands (Australia)*, *6*, 12–22.
Ball, M. C. (1988), Ecophysiology of mangroves, *Trees*, *2*, 129–142.
Ball, M. C. (1996), Comparative ecophysiology of mangrove forest and tropical lowland moist forest, in *Tropical Forest Plant Ecophysiology*, edited by S. S. Mulkey et al., pp. 461–469, Chapman and Hall, New York.
Ball, M. C., and G. D. Farquhar (1984), Photosynthetic and stomatal responses of the Grey Mangrove, *Avicennia marina*, to transient salinity conditions, *Plant Physiol.*, *74*, 7–11.
Ball, M. C., I. R. Cowan, and G. D. Farquhar (1988), Maintenance of leaf temperature and the optimisation of carbon gain in relation to water loss in a tropical mangrove forest, *Aust. J. Plant Physiol.*, *15*, 263–276.
Barr, J. G., J. D. Fuentes, V. Engel, and J. C. Zieman (2009), Physiological responses of red mangroves to the climate in the Florida Everglades, *J. Geophys. Res.*, *114*, G02008, doi:10.1029/2008JG000843.
Barr, J. G., V. Engel, J. D. Fuentes, J. C. Zieman, T. L. O'Halloran, T. J. Smith III, and G. H. Anderson (2010), Controls on mangrove forest-atmosphere carbon dioxide exchanges in western Everglades National Park, *J. Geophys. Res.*, *115*, G02020, doi:10.1029/2009JG001186.
Barr, J. G., V. Engel, T. J. Smith III, and J. D. Fuentes (2012), Hurricane disturbance and recovery of energy balance, CO_2 fluxes and canopy structure in a mangrove forest of the Florida Everglades, *Agric. For. Meteorol.*, *153*, 54–66, doi:10.1016/j.agrformet.2011.07.022.
Barr, J. G., J. D. Fuentes, M. S. DeLonge, T. L. O'Halloran, D. Barr, and J. C. Zieman (2013a), Summertime influences of tidal energy advection on the surface energy balance in a mangrove forest, *Biogeosciences*, *10*, 501–511, doi:10.5194/bg-10-501-2013.
Barr, J. G., V. Engel, J. D. Fuentes, D. O. Fuller, and H. Kwon (2013b), Modeling light use efficiency in a subtropical mangrove forest equipped with CO_2 eddy covariance, *Biogeosciences*, *10*, 2145–2158, doi:10.5194/bg-10-2145-2013.
Bouillon, S., et al. (2008), Mangrove production and carbon sinks: A revision of global budget estimates, *Global Biogeochem. Cycles*, *22*, GB2013, doi:10.1029/2007GB003052.
Choi, M., W. P. Kustas, and R. L. Ray (2012), Evapotranspiration models of different complexity for multiple land cover types, *Hydrol. Processes*, *26*, 2962–2972.
Duever, M. J., J. F. Meeder, L. C. Meeder, and J. M. McCollom (1994), The climate of south Florida and its role in shaping the Everglades ecosystem, in *Everglades: The Ecosystem and Its Restoration*, edited by S. M. Davis and J. C. Ogden, pp. 225–248, St. Lucie, Delray Beach, Fla.
Giri, C., E. Ochieng, L. L. Tieszen, Z. Zhu, A. Singh, T. Loveland, J. Masek, and N. Duke (2011), Status and distribution of mangrove forests of the world using earth observation satellite data, *Global Ecol. Biogeogr.*, *20*, 154–159, doi:10.1111/j.1466-8238.2010.00584.x.
Gu, L., et al. (2007), Influences of biomass heat and biochemical energy storages on the land surface fluxes and radiative temperature, *J. Geophys. Res.*, *112*, D02107, doi:10.1029/2006JD007425.
Heusinkveld, B. G., A. F. G. Jacobs, A. A. M. Holtslag, and S. M. Berkowicz (2004), Surface energy balance closure in an arid region: Role of soil heat flux, *Agric. For. Meteorol.*, *122*, 21–37.
Jarvis, P. G., and K. G. McNaughton (1986), Stomatal control of transpiration: Scaling up from leaf to region, in *Advances in Ecological Research*, vol. 15, edited by A. MacFadyen and E. D. Ford, pp. 1–49, Academic Press, New York.
Kumagai, T., T. M. Saitoh, Y. Sato, T. Morooka, O. J. Manfroi, K. Kuraji, and M. Suzuki (2004), Transpiration, canopy conductance and the decoupling coefficient of a lowland mixed dipterocarp forest in Sarawak, Borneo: Dry spell effects, *J. Hydrol.*, *287*, 237–251, doi:10.1016/j.jhydrol.2003.10.002.
Lundblad, M., and A. Lindroth (2002), Stand transpiration and sapflow density in relation to weather, soil moisture and stand characteristics, *Basic Appl. Ecol.*, *3*, 229–243.
McNaughton, K. G., and P. G. Jarvis (1983), Predicting effects of vegetation changes on transpiration and evaporation, in *Water Deficits and Plant Growth*, vol. VII, edited by T. T. Kozlowski, pp. 1–47, Academic Press, New York.
McNaughton, K. G., and P. G. Jarvis (1991), Effects of spatial scale on stomatal control of transpiration, *Agric. For. Meteorol.*, *54*, 279–301.
Monteith, J. L. (1995), Accomodation between transpiring vegetation and the convective boundary layer, *J. Hydrol.*, *166*, 251–263.
Monteith, J. L., and M. H. Unsworth (2013), *Principles of Environmental Physics*, 4th ed., Academic Press, Oxford, U. K.
Murray, F. W. (1967), On the computation of saturation vapor pressure, *J. Appl. Meteorol.*, *6*, 203–204.
Parida, A. K., and B. Jha (2010), Salt tolerance mechanisms in mangroves: A review, *Trees*, *24*, 199–217, doi:10.1007/s00468-010-0417-x.
Passioura, J. B., M. C. Ball, and J. H. Knight (1992), Mangroves may salinize soil and in so doing limit their transpiration rate, *Funct. Ecol.*, *6*(4), 476–481.
Priestley, C. H. B., and R. J. Taylor (1972), On the assessment of surface heat flux and evaporation using large-scale parameters, *Mon. Weather Rev.*, *100*, 81–92.
Ryu, Y., D. D. Baldocchi, S. Ma, and T. Hehn (2008), Interannual variability of evapotranspiration and energy exchange over an annual grassland in California, *J. Geophys. Res.*, *113*, D09104, doi:10.1029/2007JD009263.
Sperry, J. S., M. T. Tyree, and J. R. Donnelly (1988), Vulnerability of xylem to embolism in a mangrove vs. an inland species of *Rhizophoraceae*, *Physiol. Plant.*, *74*, 276–283.
Tetens, O. (1930), Über einige meteorologische Begriffe, *Z. Geophys.*, *6*, 297–309.
Twine, T. E., W. P. Kustas, J. M. Norman, D. R. Cook, P. R. Houser, T. P. Meyers, J. H. Pueger, P. J. Starks, and M. L. Wesely (2000), Correcting eddy-covariance flux underestimates over a grassland, *Agric. For. Meteorol.*, *103*, 279–300.
Wilson, K. B., and D. D. Baldocchi (2000), Seasonal and interannual variability of energy fluxes over a broadleaved temperate deciduous forest in North America, *Agric. For. Meteorol.*, *100*, 1–18.